



## 저작자표시-비영리-변경금지 2.0 대한민국

이용자는 아래의 조건을 따르는 경우에 한하여 자유롭게

- 이 저작물을 복제, 배포, 전송, 전시, 공연 및 방송할 수 있습니다.

다음과 같은 조건을 따라야 합니다:



저작자표시. 귀하는 원저작자를 표시하여야 합니다.



비영리. 귀하는 이 저작물을 영리 목적으로 이용할 수 없습니다.



변경금지. 귀하는 이 저작물을 개작, 변형 또는 가공할 수 없습니다.

- 귀하는, 이 저작물의 재이용이나 배포의 경우, 이 저작물에 적용된 이용허락조건을 명확하게 나타내어야 합니다.
- 저작권자로부터 별도의 허가를 받으면 이러한 조건들은 적용되지 않습니다.

저작권법에 따른 이용자의 권리는 위의 내용에 의하여 영향을 받지 않습니다.

이것은 [이용허락규약\(Legal Code\)](#)을 이해하기 쉽게 요약한 것입니다.

[Disclaimer](#)

Master's Thesis

Time-resolved spectroscopic study of dual  
heteroatom-doped carbon dots

Sunghu Kim

Department of Chemistry

Graduate School of UNIST

2017

# Time-resolved spectroscopic study of dual heteroatom-doped carbon dots

Sunghu Kim

Department of Chemistry

Graduate School of UNIST

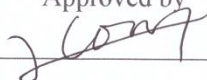
Time-resolved spectroscopic study of dual  
heteroatom-doped carbon dots

A thesis/dissertation  
submitted to the Graduate School of UNIST  
in partial fulfillment of the  
requirements for the degree of  
Master of Science

Sunghu Kim

12. 15. 2016

Approved by



Advisor

Oh-Hoon Kwon

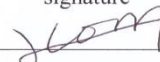
Time-resolved spectroscopic study of dual  
heteroatom-doped carbon dots

Sunghu Kim

This certifies that the thesis/dissertation of Sunghu Kim is approved.

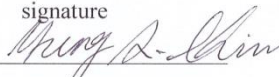
12/15/2016

signature



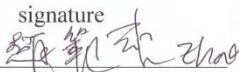
Advisor: Oh-Hoon kwon

signature



Prof. Yung Sam Kim

signature



Prof. Bum Suk Zhao

## Abstract

Carbon dots (CDs) have a potential application in bioimaging due to their excellent photoluminescence (PL), nontoxicity, and excitation-dependent photoluminescence (PL). We studied time-resolved spectroscopic behavior of nitrogen-doped carbon dots (N-CD) and boron-nitrogen doped carbon dots (BN-CD) which were synthesized by one-step microwave pyrolysis. The PL quantum yield of BN-CD was found to be 80.8%, which is approximately twice that of N-CD (40.2%). Although several PL mechanisms of CDs have been proposed in many reports, the origin of the PL of CDs is still in debate. We investigated the origin of the PL of CDs by using a series of spectroscopic methods. The PL lifetimes were fitted by stretched exponential functions which can generally describe to surface-functional PL systems having a distribution of chromophoric states. As a result, we observed that both the CDs pose multiple surface-functional electronic states with a dominant molecular-like state. This study successfully demonstrates the application of stretched exponential functions in describing heterogeneous PL systems.

## Contents

I. Introduction -----	5
II. Method and Materials -----	7
III. Results and Discussion -----	7
3.1 Steady-state absorption and emission spectra -----	7
3.2 X-ray photoelectron spectroscopic measurement -----	8
3.3 Time-resolved spectroscopic analysis -----	8
IV. Conclusion -----	11
V. Figures, Schemes and Tables -----	12
VI. References -----	24
VII. Acknowledgements -----	29

## List of Figures

**Figure 1.** Optical spectra of CDs in an aqueous solution. Absorption spectrum (black solid line), excitation spectrum (red solid line), and PL spectra (blue solid and dashed line) of (a) N-CD and (b) BN-CD. Emission spectra were measured by excitation at 250 nm (blue dashed line) and 350 nm (blue solid line). Excitation spectra were measured by emission at 450 nm. Insets show the magnified PL spectra with excitation at 250 nm.

**Figure 2.** (a) PL spectra of N-CD with varying excitation wavelengths from 310 to 450 nm with 20 nm increments. (b) Excitation spectra of N-CD with varying emission wavelengths from 410 to 550 nm with 20 nm increments.

**Figure 3.** (a) PL spectra of BN-CD with varying excitation wavelengths from 310 to 450 nm with 20 nm increments. (b) Excitation spectra of BN-CD with varying emission wavelengths from 410 to 550 nm with 20 nm increments.

**Figure 4.** Fluorescence decay profiles of N-CD (left panels) and BN-CD (right panels) with excitation at 375 nm monitored at (a) 450 nm, (b) 500 nm, (c) 550 nm, and (d) 600 nm, respectively.

**Figure 5.** (a) Time-resolved emission spectra (TRES) of N-CD with excitation wavelength at 375 nm. Fitting parameters are given according to stretched exponential functions (b-d). (b) The amplitudes of fluorescence lifetime components of N-CD. (c) Stretched exponential distribution factor,  $\beta$ , of N-CD. (d) Fluorescence lifetimes of N-CD. All decay transients were taken from 400 to 650 nm with 5 nm increments. Inset shows the normalized spectra.

**Figure 6.** (a) Time-resolved emission spectra (TRES) of BN-CD with excitation wavelength at 375 nm. Fitting parameters are given according to stretched exponential functions (b-d). (b) The amplitudes of fluorescence lifetime components of BN-CD. (c) Stretched exponential distribution factor,  $\beta$ , of BN-CD. (d) Fluorescence lifetimes of BN-CD. All decay transients were taken from 400 to 650 nm with 5 nm increments. Inset shows the normalized spectra.

**Figure S1.** (a) Normalized PL spectra of N-CD with varying excitation wavelengths from 310 to 450 nm with 20 nm increments. (b) Normalized excitation spectra of N-CD with varying emission wavelengths from 410 to 550 nm with 20 nm increments.



**Figure S2.** (a) Normalized PL spectra of BN-CD with varying excitation wavelengths from 310 to 450 nm with 20 nm increments. (b) Normalized excitation spectra of BN-CD with varying emission wavelengths from 410 to 550 nm with 20 nm increments.

**Figure S3.** Time-resolved area normalized emission spectra (TRANES) of (a) N-CD and (b) BN-CD.

**Figure S4.** High-resolution XPS spectra C 1s and N 1s of (a,c) N-CD and (b,d) BN-CD, respectively.

## List of Tables

**Table 1.** Fitting parameters of PL decay of N-CD with excitation at 375 nm.

**Table 2.** Fitting parameters of PL decay of BN-CD with excitation at 375 nm.

## List of Schemes

**Scheme 1.** Proposed PL mechanism of both CDs.

## Explanation of abbreviations

CDs	- Carbon dots
N-CD	- Nitrogen doped carbon dots
BN-CD	- Boron and nitrogen carbon dots
PL QY	- Photoluminescence quantum yield
CA	- Citric acid
EDA	- Ethylenediamine
XPS	- X-ray photoelectron spectroscopy
TRES	- Time-resolved emission spectra

## Introduction

Carbon nanomaterials such as fullerene,<sup>1</sup> carbon nanotube,<sup>2</sup> graphene,<sup>3</sup> carbon dots (CDs)<sup>4</sup> are promising in nanotechnology due to their unique physical and chemical properties. Carbon dots (CDs) are a new class of the carbon nanomaterials which have commonly below a 10 nm size. CDs generally consist of graphitic structure in few layers and various organic functional groups on the surface of CDs.

CDs have advantages of their unique properties such as excellent photoluminescence (PL), biocompatibility, and high photostability. One of the most advantages of CDs is non-toxicity because heavy metal is not included in CDs as compared with inorganic quantum dots such as CdSe and ZnO.<sup>5-6</sup> In these advantages, CDs can be applied in optoelectronics,<sup>7-8</sup> bioimaging,<sup>9-10</sup> photocatalyst,<sup>11</sup> biosensor,<sup>12</sup> drug delivery<sup>13</sup> and solar light harvesting,<sup>14</sup> *etc.*

The PL quantum yield (PL QY) of CDs is a key parameter for preparing strong fluorescent materials. However, PL QY of CDs is commonly low without chemical modification.<sup>15</sup> So, many studies have been reported to enhance the PL QY of CDs by doping heterogeneous atoms, reduction on the surface, surface passivation, adopting different synthetic conditions and/or using various precursors.<sup>16-22</sup>

The various synthetic routes have been developed in bottom-up and top-down approaches to enhance the performance of luminescence of CDs. The top-down method is a cutting procedure through electrochemical,<sup>23-25</sup> laser ablation,<sup>26-31</sup> and arc charge from bulk carbon materials.<sup>32</sup> The bottom-up process is a synthetic route to build CDs from a small molecule using various organic precursors. The hydrothermal,<sup>33-34</sup> pyrolysis,<sup>17</sup> and microwave-assisted methods<sup>35-36</sup> are generally adopted as the bottom-up process due to the facile synthetic routes. Hongyang Fan & Zaicheng Sun *et al.* reported that the highest PL QY of graphene quantum dots (GQDs) was measured up to 94% through a hydrothermal method using various nitrogen precursors.<sup>16</sup>

As compared to conventional fluorescent dye, CDs have unique optical properties due to their PL depending on excitation wavelengths. To reveal the origin of this phenomenon, many researchers have studied for many years by means of surface passivation,<sup>9-10, 17, 37-38</sup> adopting different synthetic methods,<sup>39-40</sup> changing synthetic conditions,<sup>20, 41-42</sup> pH,<sup>43-45</sup> and chemical reduction,<sup>46-47</sup> *etc.* However, the origin of the PL of the CDs is still debated in current status. The several mechanisms of the PL behaviors of carbon materials including CDs have been proposed; abundant chemical functional

groups on the CDs surface,<sup>41, 48-49</sup> quantum confinement effects,<sup>29, 50-51</sup> electron-hole localized states due to the oxygen-related functional groups,<sup>47, 52</sup> and molecular-like state,<sup>37, 39, 42, 53-54</sup> *etc.* Bhattacharya *et al.* observed that CDs show the wide size distribution from AFM profile.<sup>50</sup> They concluded that an excitation-dependent PL behavior of CDs originates from the quantum confinement effect rather than the distribution of different surface trap states. Pang *et al.* prepared CDs with different degree of surface oxidation by electrochemical method.<sup>41</sup> They suggested that the excitation-dependent PL of CDs was attributed to the oxygen-related surface states. Yang *et al.* prepared CDs by a hydrothermal route using a citric acid and ethylenediamine (EDA) as the precursors.<sup>54</sup> They observed that the fluorescent molecules (imidazo[1,2-*a*]pyridine-7-carboxylic acid, 1,2,3,5-tetrahydro-5-oxo-, IPCA) were found to be in CDs. They suggested that IPCA molecules which are called to the molecular states contribute the strong blue emission of CDs.

Here, we synthesized the boron-and-nitrogen co-doped CDs (BN-CDs) thorough a single-step microwave route using citric acid (CA), ethylenediamine (EDA), and boric acid as the precursors.<sup>15</sup> BN-CD has a novel type of dual heteroatom-doped carbon dots which have high photostability and excellent PL as compared with plain carbon dots (CDs) and nitrogen-doped carbon dots (N-CDs). The PL QY of BN-CD (80.8%) is twice as compared to that of N-CD (40.2%) due to having their different nitrogen configuration.<sup>15</sup> Aforementioned, the photoluminescence mechanism is still open debate. We analyzed the series of spectroscopic results by using X-ray photoelectron spectroscopy (XPS), UV-vis spectroscopy, photoluminescence (PL) and time-resolved electronic spectroscopy to reveal the origin of photoluminescence mechanism. We also suggested that the CDs have mainly two components of PL with the heterogeneous systems (multiple electronic states) and a dominant homogeneous system (molecular-like state) according to a stretched exponential function.

## Methods and Materials

Nitrogen-doped carbon dots (N-CD) have synthesized microwave pyrolysis routes which performed in presence of a citric acid and EDA as the precursors. Boron and nitrogen doped carbon dots (BN-CD) are also prepared by a microwave pyrolysis method in presence of a citric acid, an ethylenediamine, and a boric acid as the precursors. Both CDs are prepared by Dr. Yuri Choi.<sup>15</sup> The structural analysis of CDs was obtained using a X-ray photoelectron spectroscopy (K-alpha, Thermo Fisher), these data were also measured by Dr. Yuri Choi.<sup>15</sup> UV-vis spectra were obtained by using a UV-vis spectrometer (V-730, Jasco) and steady-state fluorescence spectra were obtained by using a fluorometer instrument (Shimadzu 6000). PL lifetimes were measured by a time-correlated single photon counting spectrometer (Fluotime 300, PicoQuant) with the light source of picosecond-pulsed diode lasers emitting at 375 nm (LDH-D-C-375, PicoQuant). The total instrument response function (IRF) was ~190 ps. All fluorescence decay profiles were fitted to stretched exponential function exponential functions by using the software (FluoFit, PicoQuant) to deduced fluorescence lifetimes.

## Results and Discussion

### 1. Steady-state absorption and emission spectra

The optical characterization of both the CDs was investigated in this study (**Figure 1**). Absorption peaks were found to be at ~250 nm and ~350 nm in both CDs which are generally assigned to  $\pi$ - $\pi^*$  and  $n$ - $\pi^*$  transition corresponding to the  $sp^2$  carbon core transition and the transition of the surface functional groups, respectively.<sup>16, 19, 37, 53, 55-56</sup> In addition, nitrogen doped carbon dots (N-CD) absorb the light over the visible range at ~420 nm, indicating of presence of multiple electronic states whereas there is no absorption tail in boron-nitrogen doped CDs (BN-CD). The PL maximum of both CDs features at ~450 nm with excitation at 350 nm, and their PL excitation spectrum also found to be at ~250 and ~350 nm under emission wavelength at 450 nm. Inset shows the PL spectrum with weak shoulder at ~330 nm under excitation at 250 nm which is related to transition of carbon core. The reason that PL intensity at ~330 nm is very weak as compared to the peak at ~450 nm maybe due to the energy transfer. The PL spectra of N-CD showed an excitation-dependent behavior due to having the multiple electronic states on the surface of CDs (**Figures 2a, S1a**). The PL excitation spectra of N-CD found to be at ~250 nm, ~360 nm, ~450 nm, and ~510 nm (**Figures 2b, S1b**). However, the maximum of the PL of the BN-CD was centered at ~450 nm which was independent on excitation wavelengths in contrast to that of N-CD (**Figures 3a, S2a**). In addition, the PL excitation spectra of BN-CD feature the bands at ~250 nm and ~350 nm (**Figure 3b, S2b**). These bands were also found in N-CD, whereas the bands at ~450 nm and ~510 nm were suppressed in BN-CD. In basis of our results, the bands over the visible range at ~450 nm in PL excitation spectra lead to an excitation-dependent

PL behavior. As our best knowledge, the excitation-dependent PL of CDs is generally accepted due to the oxygen-related surface functional groups which can form multiple electronic states.<sup>17, 41</sup>

## 2. X-ray photoelectron spectroscopic measurement

To analyze of the chemical compositions of both the CDs, X-ray photoelectron spectroscopy (XPS) were performed (**Figure S4**). The major elements of both CDs consisted C, N, and O. In the high resolution C 1s spectra, the fractions of carbon-related bonding with N and O species were different between N-CD and BN-CD. The fit results were summarized in BN-CD: C=C (284.74 eV), C=O (287.92 eV), C-N (285.77 eV) and COOH (288.79 eV). As compared to N-CD, the fractions of C=C and C=O were increased whereas that of COOH and C-N were reduced in BN-CD. Interestingly, the N 1s spectra show the different nitrogen configurations between N-CD and BN-CD. N-CD possess dominantly pyrrolic-N, whereas the BN-CD mainly consists of graphitic-N. On the basis of these results, the nitrogen configurations play important role of their PL behavior. We suggest that the pyrrolic-N caused the formation of the nitrogen-related defect states, however, the graphitic-N enhanced the conjugation of sp<sup>2</sup>-related carbon domains. Zou *et al.* also suggested that the nitrogen defect can form the absorption tail over the visible range at ~450 nm and excitation-dependent PL.<sup>57</sup> Therefore, the PL QY of BN-CD (80.8%) is nearly twice as compared to that of N-CD (40.2%).<sup>15</sup>

## 3. Time-resolved spectroscopic analysis

We obtained time-resolved PL decay profiles of both the CDs using a time-correlated single photon counting (TCSPC). The PL decay transients of N-CD show more dependent PL decay time with monitored wavelengths as compared to those of BN-CD (**Figure 4**). In other words, the PL decay time was shortened as increasing the emission wavelength due to their emissive states on the surface of CDs, whereas the PL decay time of BN-CD is independent on emission wavelengths that means the surface electronic states of BN-CD is less having than that of N-CD. We investigated to deeply understand the origin of the PL of both the CDs, all decay curves were fitted by multiple stretched exponential functions as following equation.

$$I(t) = \sum_{i=1}^n A_i \exp\left(-\frac{t}{\tau_i}\right)^{\beta_i}$$

The stretched exponential function is commonly used for disordered relaxation systems which are introduced in CDs due to their complicated luminophores. Here, we presented the stretched exponential decay parameters; PL lifetimes ( $\tau$ ), fractional amplitudes of fluorescence lifetime components and  $\beta$  which is distribution of PL lifetimes where a smaller  $\beta$  means a wider distribution of PL lifetimes (**Tables 1,2**). According to the stretched exponential parameters in N-CD, the PL

lifetimes were found to be 12-15 ns ( $\tau_1$ ) and 500 ps-3 ns ( $\tau_2$ ) which correspond the values of  $\beta$  with  $\sim 1.0$  ( $\beta_1$ ) and 0.5-0.8 ( $\beta_2$ ), respectively. The PL lifetimes in BN-CD are also obtained to be  $\sim 15$  ns ( $\tau_1$ ) and 400 ps-2 ns ( $\tau_2$ ) which presented the values of  $\beta$  with  $\sim 1.0$  ( $\beta_1$ ) and  $\sim 0.3$  ( $\beta_2$ ), respectively. The fractional amplitudes of  $\tau_1$  are dominant at 450 nm in both CDs which found to be 0.76 and 0.93 in N-CD and BN-CD, respectively. As increasing the emission wavelength, the fractional amplitude of  $\tau_1$  is decreased and that of  $\tau_2$  increased in both the CDs. The PL lifetimes of  $\tau_1$  are similar between N-CD and BN-CD. The PL lifetimes of  $\tau_1$  were already reported to the lifetime of IPCA molecule.<sup>54</sup> Nann *et al.* also reported that the fitting of PL lifetimes of graphene quantum dots were mainly found two systems, a homogeneous with fluorescein dye and a highly heterogeneous system.<sup>58</sup> The values of other PL lifetimes ( $\tau_2$ ) in both CDs are varied with the emission wavelengths and the values of  $\beta$  are also smaller than 1.0 that means these components originate from heterogeneous electronic systems. We suggest that heterogeneous electronic systems come from surface functional groups of the CDs. As the basis of the results, the molecular states dominantly contribute their strong blue emission and the surface functional groups can form disordered electronic states of the CDs.

To find the emitting species of the CDs, we obtained time-resolved emission spectra (TRES) from 400 to 650 nm with 5-nm increments. The spectral maximum is found at  $\sim 450$  nm in both the CDs with excitation at 375 nm (**Figures 5a, 6a**). In time-resolved area normalized spectra (TREANS), there were neither spectra shifts nor isoemissive points at varying time delays in both the CDs (**Figure S3**).

All kinetic profiles at  $\lambda_{em} = 400$ -650 nm were also fitted by multiple stretched exponential functions in both the CDs. The distribution of fitting parameters with amplitudes of each PL lifetime component ( $A_i$ ), distribution of PL lifetimes,  $\beta_i$ , and their PL lifetimes ( $\tau_i$ ) are given in the whole range of wavelengths (400-650 nm) in both the CDs (**Figures 5b-d, 6b-d**).  $A_1$  is found to be at  $\sim 450$  nm and it has dominant contribution in both the CDs. This amplitude in both the CDs corresponds the values of  $\beta_1$  and  $\tau_1$  with  $\sim 15$  ns and  $\sim 1.0$ , respectively. The dominant amplitude originates from molecular states because this component matches well the PL lifetime of the IPCA and homogeneous systems ( $\beta_1 = \sim 1.0$ ). On the other hand, the contribution of  $A_2$  is more dominant in N-CD as compared to that of BN-CD. Furthermore, the N-CD has the values of  $\beta_2$  at  $\sim 0.6$  and disordered distribution of the PL lifetimes in the whole range of wavelengths. However, the BN-CD has the values of  $\beta_2$  at  $\sim 0.3$  and well distributed PL lifetimes at  $\sim 400$  ps. According to these results, the values of  $\beta_2$  are smaller in BN-CD whereas the PL lifetimes with  $\tau_2$  are more randomly distributed in N-CD. Interestingly, the values of  $\beta_1$  and  $\tau_1$  are slightly disordered only in N-CD at the longer wavelengths from  $\sim 550$  nm. However, These values are constant in BN-CD at the whole range of wavelengths. We suggest that the disordered PL lifetimes are due to multiple chemical chromophores on the surface of CDs and the

values of  $\beta$  mean the distribution of the relaxation channels on each chemical chromophore. According to our proposed PL mechanism, Although the BN-CD has less chemical chromophores as compared to that of N-CD, BN-CD has more relaxation channels on each chemical chromophore than that of N-CD. The reason of having variable relaxation channels in BN-CD is due to local environment effect on their chemical chromophores which maybe originate from the conjugation systems on the carbon core, surface electronic localized states,  $sp^3$  carbon defect and so on.

Our summarized PL mechanism of both the CDs is shown (**Scheme 1**). Carbon core domains are excited at  $\sim 250$  nm, and their emission at  $\sim 330$  nm which is very weak due to the fast energy transfer to a dominant molecular state. The maximum of molecular states is found to be  $\sim 450$  nm and their absorption at  $\sim 350$  nm. The PL lifetime is estimated to be  $\sim 15$  ns at  $\sim 450$  nm in both CDs, and the lifetime is well defined ( $\beta = \sim 1.0$ ) as that of IPCA. The surface states are excited above 420 nm and their PL is dependent on chemical chromophoric states. The absorption tail featured only N-CD beyond the  $\sim 420$  nm and excitation spectra show the bands at  $\sim 450$  nm and  $\sim 510$  nm. N-CD has the various PL lifetimes ( $\sim 200$  ps-3 ns) on surface of CDs that means the multiple chemical chromophoric states and results in excitation-dependent PL. On the other hand, BN-CD has the well distributed PL lifetimes ( $\sim 400$  ps) on the surface of CDs that means having less surface chemical chromophores. The well distributed PL lifetimes lead to the excitation-independent PL behavior. Instead, the values of  $\beta$  are smaller in BN-CD as compared to that of N-CD. We suggest that the BN-CD has more relaxation channels on each chemical chromophore as compared to that of N-CD. According to the chemical composition of the CDs, N-CD has dominant functional groups with  $-\text{COOH}$  and pyrrolic-N whereas the BN-CD pose abundant function groups with graphitic-N. The functional groups of  $-\text{COOH}$  and pyrrolic-N form the multiple chemical chromophores which lead to the excitation-dependent PL behaviors. We concluded that the chemical composition on the surface of CDs can affect the excitation-dependent PL behavior.

## Conclusion

In summary, the PL mechanisms of the CDs have been proposed with various points of view for few years. However, the origin of the PL of the CDs is still debated and unclear. We investigated the PL mechanism of the CDs by analyzing the series of spectroscopic measurements with steady-state absorption and emission spectra, time-resolved PL, and using a X-ray photoelectron spectroscopy (XPS). The PL behavior of N-CD is dependent on excitation wavelengths whereas that of BN-CD is independent on excitation wavelengths. We observed that the different nitrogen configuration between N-CD and BN-CD is a key role of an excitation-dependent PL behavior and results in their different values of PL QY. To deeply understand their PL mechanisms, the PL lifetimes of both the CDs were fitted by stretched exponential functions due to their complicated electronic states. CDs pose the two electronic states which are homogeneous PL system and heterogeneous PL system with a dominant molecular-like state and multiple surface functional electronic states. Molecular-like states dominantly affect their strong blue emission with PL lifetime at ~15 ns which correspond to the PL lifetime of IPCA. The multiple surface functional electronic states contribute their excitation-dependent PL behaviors. We believe that this study will help understand the origin of the PL of carbon nanomaterials in future perspective.



## Figures, Schemes and Tables

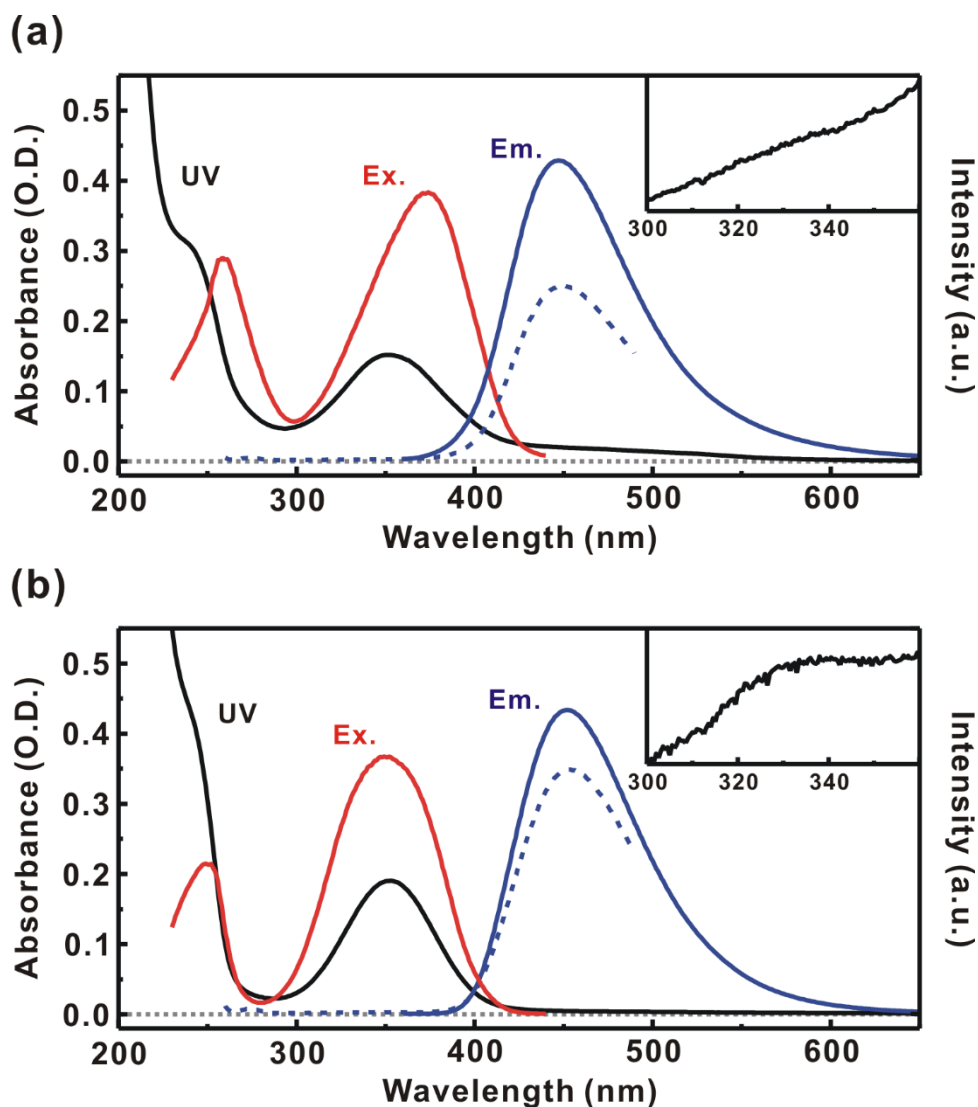


**Figure 1.** Optical spectra of CDs in an aqueous solution. Absorption spectrum (black solid line), excitation spectrum (red solid line), and PL spectra (blue solid and dashed line) of (a) N-CD and (b) BN-CD. Emission spectra were measured by excitation at 250 nm (blue dashed line) and 350 nm (blue solid line). Excitation spectra were measured by emission at 450 nm. Insets show the magnified PL spectra with excitation at 250 nm.

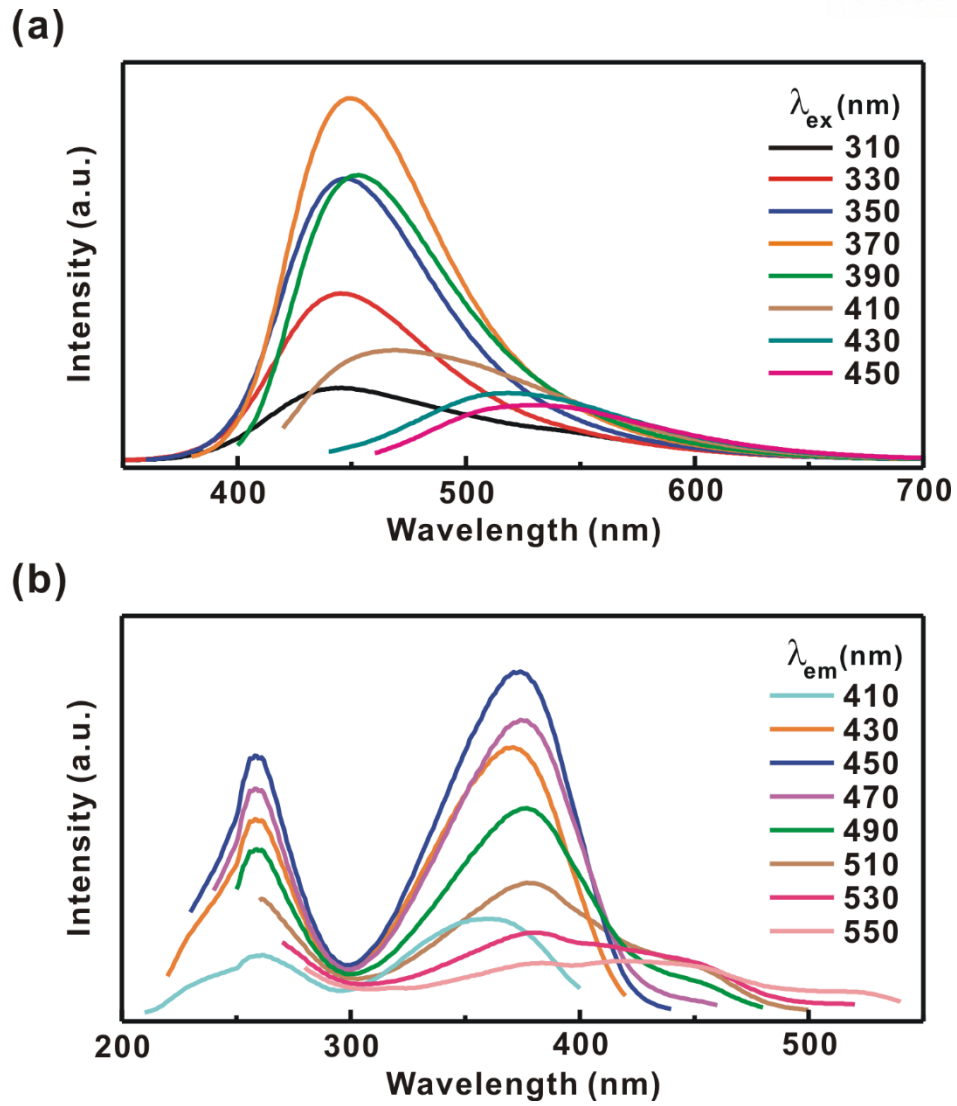


**Figure 2.** (a) PL spectra of N-CD with varying excitation wavelengths from 310 to 450 nm with 20 nm increments. (b) Excitation spectra of N-CD with varying emission wavelengths from 410 to 550 nm with 20 nm increments.

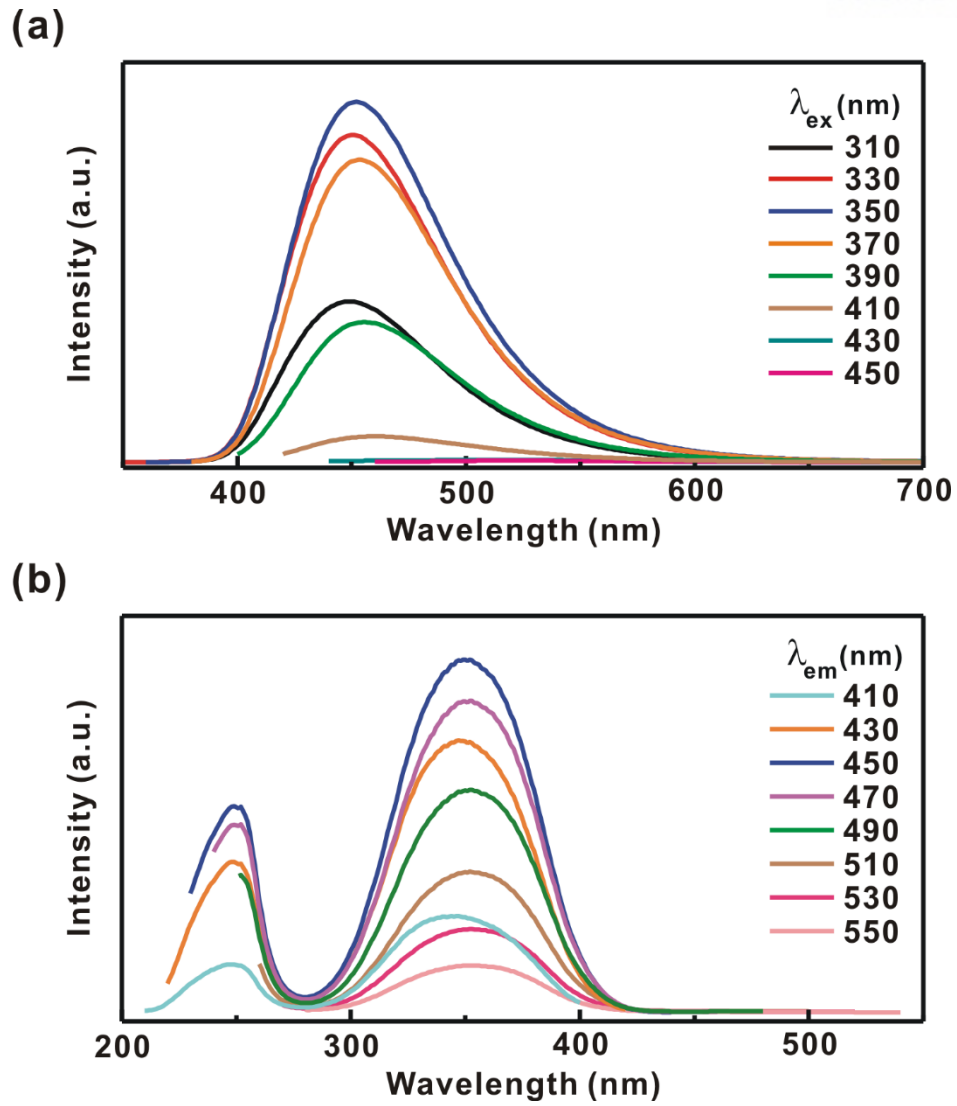


**Figure 3.** (a) PL spectra of BN-CD with varying excitation wavelengths from 310 to 450 nm with 20 nm increments. (b) Excitation spectra of BN-CD with varying emission wavelengths from 410 to 550 nm with 20 nm increments.

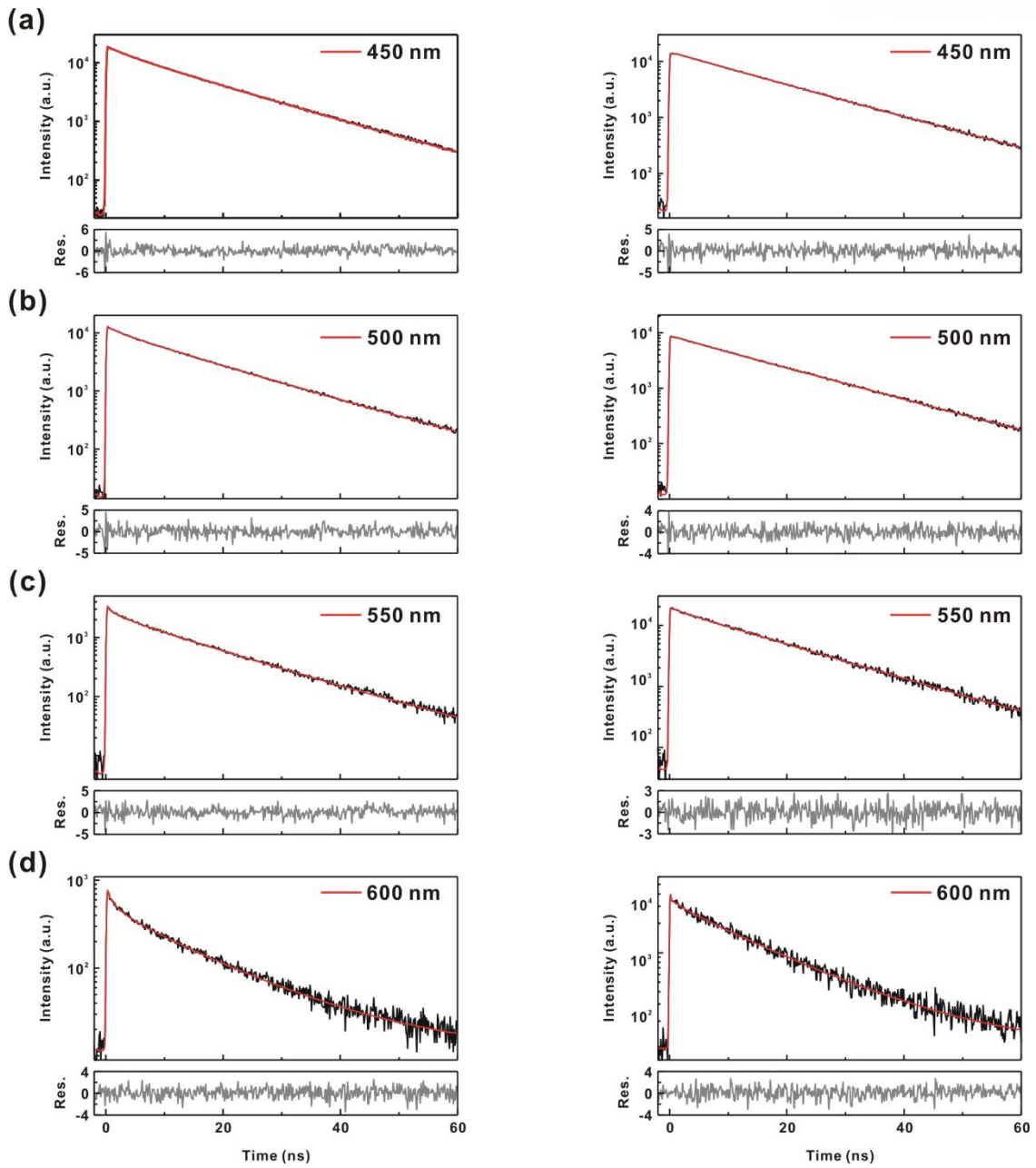


**Figure 4.** Fluorescence decay profiles of N-CD (left panels) and BN-CD (right panels) with excitation at 375 nm monitored at (a) 450 nm, (b) 500 nm, (c) 550 nm, and (d) 600 nm, respectively.

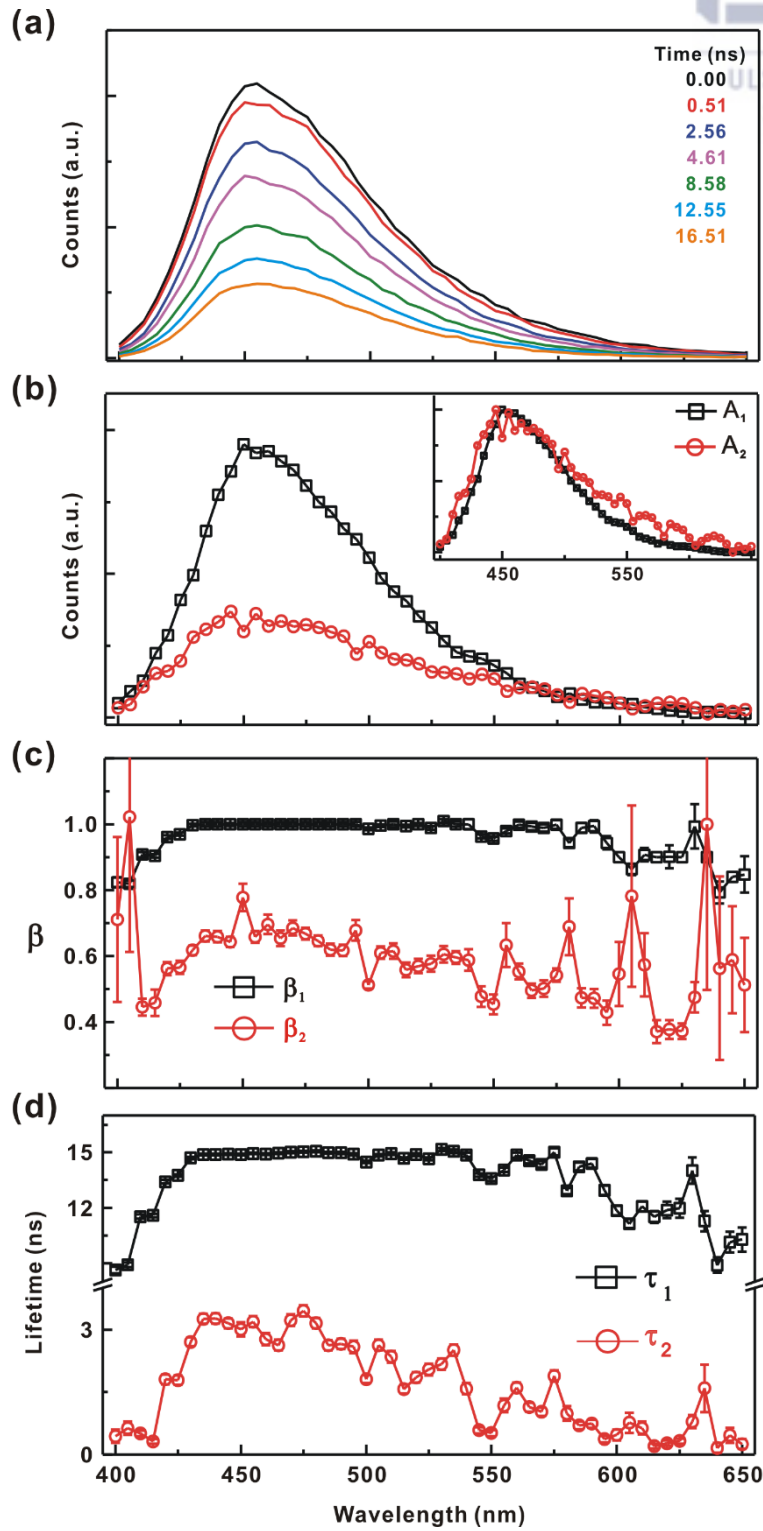


**Figure 5.** (a) Time-resolved emission spectra (TRES) of N-CD with excitation wavelength at 375 nm. Fitting parameters are given according to stretched exponential functions (b-d). (b) The amplitudes of fluorescence lifetime components of N-CD. (c) Stretched exponential distribution factor,  $\beta$ , of N-CD. (d) Fluorescence lifetimes of N-CD. All decay transients were taken from 400 to 650 nm with 5 nm increments. Inset shows the normalized spectra.

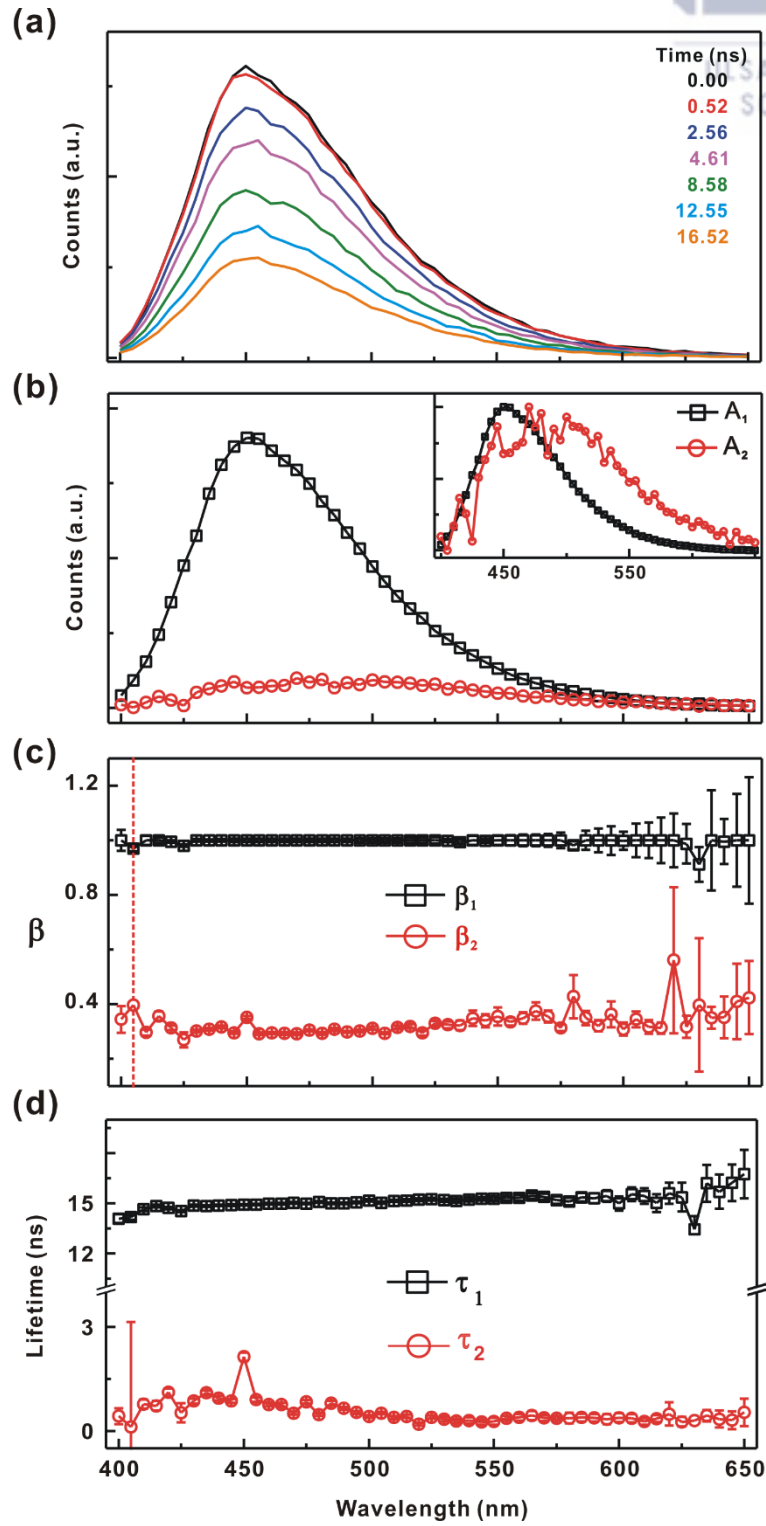


**Figure 6.** (a) Time-resolved emission spectra (TRES) of BN-CD with excitation wavelength at 375 nm. Fitting parameters are given according to stretched exponential functions (b-d). (b) The amplitudes of fluorescence lifetime components of BN-CD. (c) Stretched exponential distribution factor,  $\beta$ , of BN-CD. (d) Fluorescence lifetimes of BN-CD. All decay transients were taken from 400 to 650 nm with 5 nm increments. Inset shows the normalized spectra.

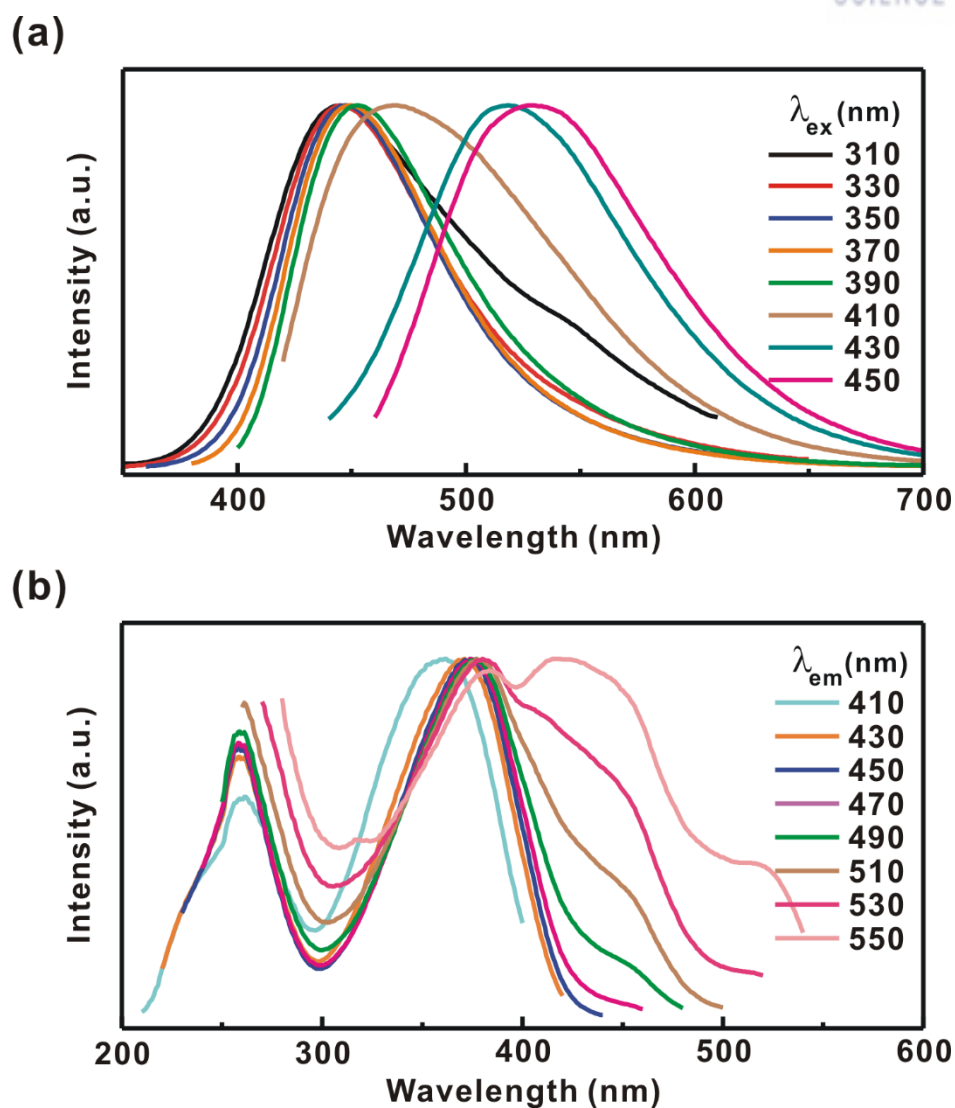


**Figure S1.** (a) Normalized PL spectra of N-CD with varying excitation wavelengths from 310 to 450 nm with 20 nm increments. (b) Normalized excitation spectra of N-CD with varying emission wavelengths from 410 to 550 nm with 20 nm increments.

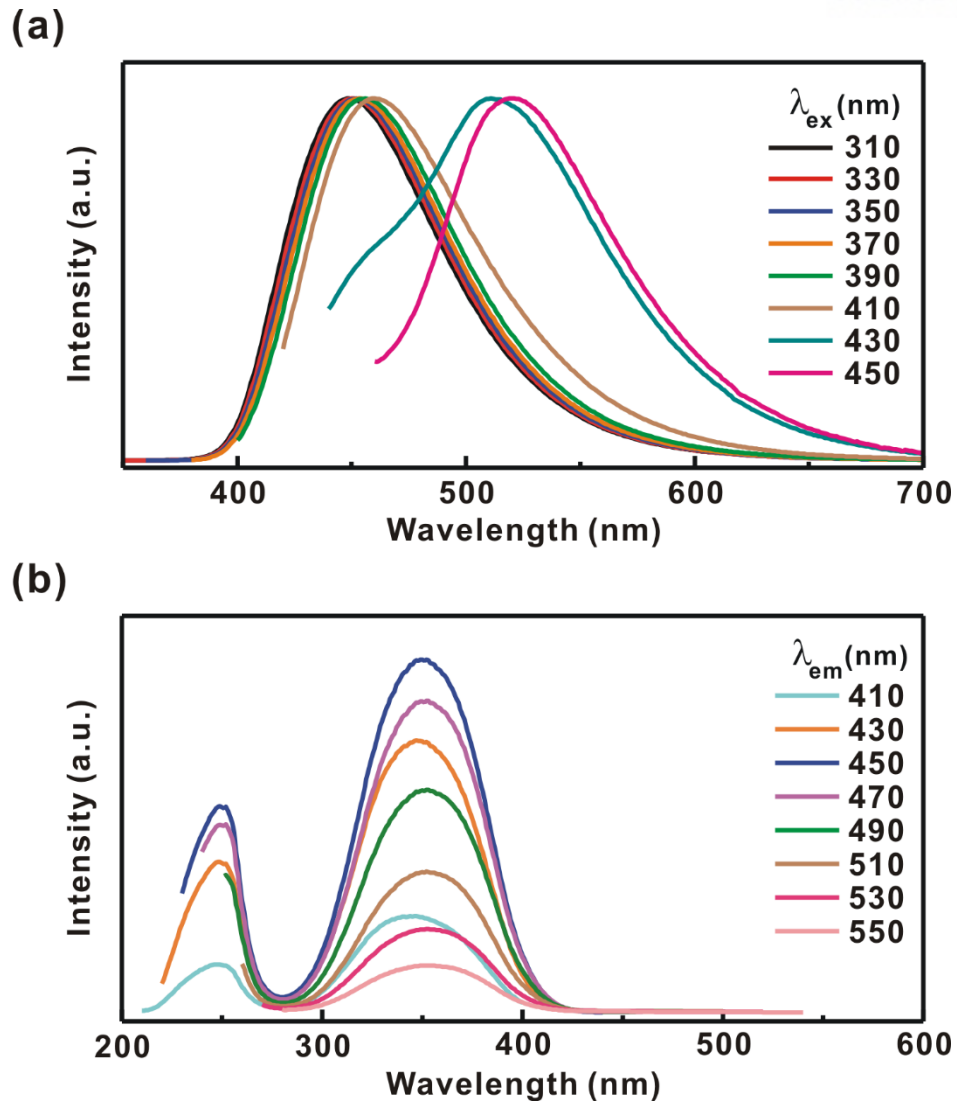


**Figure S2.** (a) Normalized PL spectra of BN-CD with varying excitation wavelengths from 310 to 450 nm with 20 nm increments. (b) Normalized excitation spectra of BN-CD with varying emission wavelengths from 410 to 550 nm with 20 nm increments.



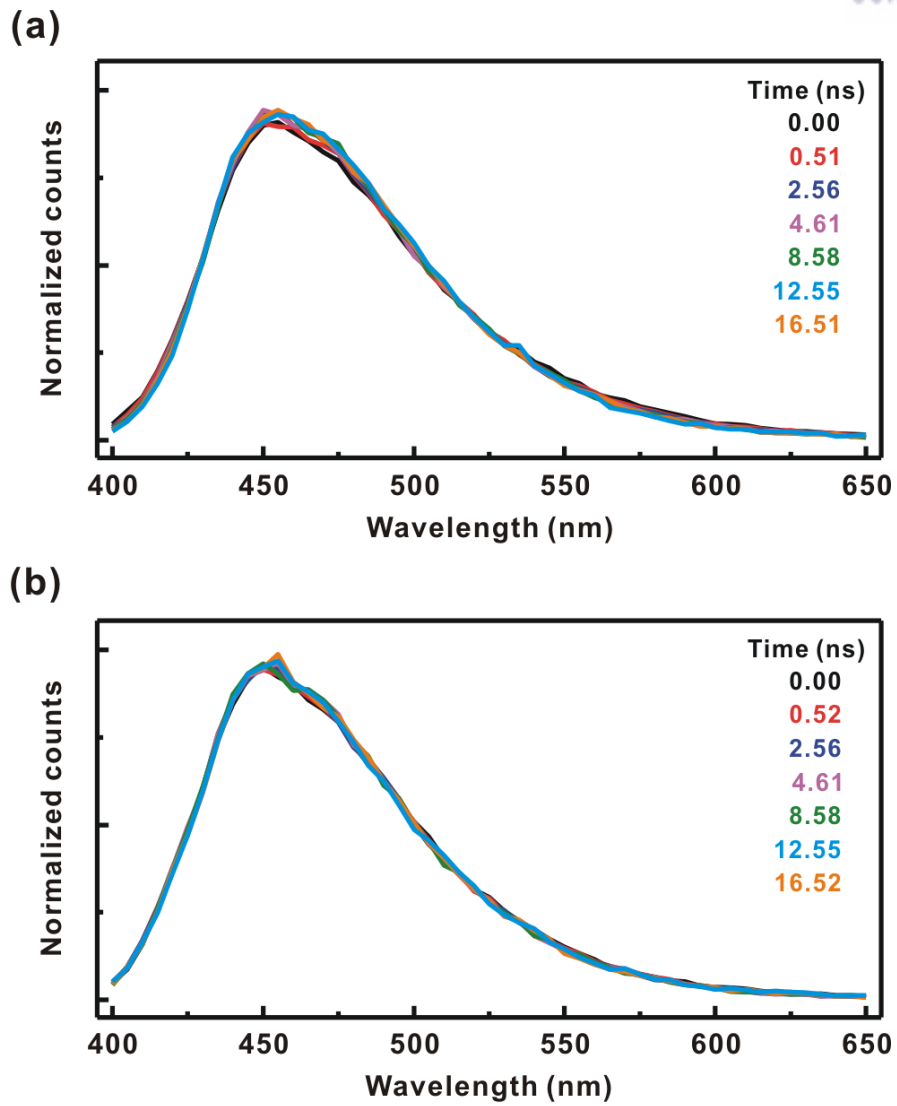


**Figure S3.** Time-resolved area normalized emission spectra (TRANES) of (a) N-CD and (b) BN-CD.

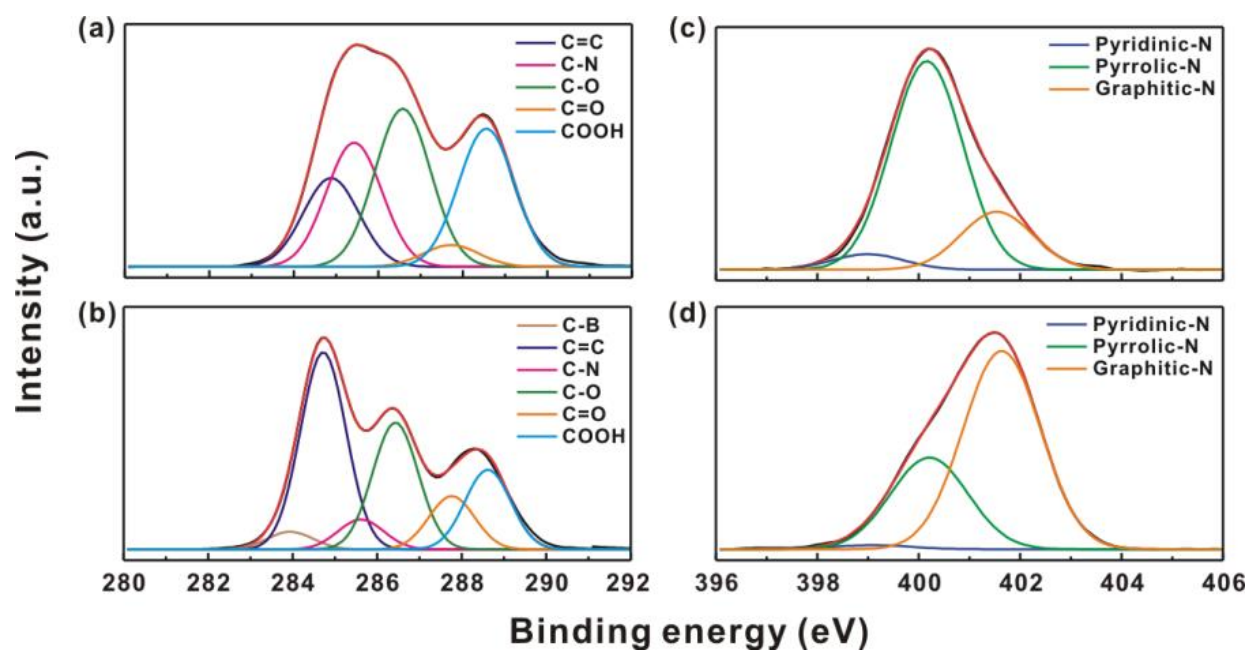


**Figure S4.** High-resolution XPS spectra C 1s and N 1s of (a,c) N-CD and (b,d) BN-CD, respectively.

**Table 1.** Fitting parameters of PL decay of N-CD with excitation at 375 nm.

N-CD					
$\lambda_{\text{em}}$ (nm)	$\tau_1$ (ns)	$\beta_1$	$\tau_2$ (ns)	$\beta_2$	$\chi^2$
450	$14.87 \pm 0.05$ (76%) <sup>a</sup>	$1.00^b$	$3.01 \pm 0.17$ (24%)	$0.78 \pm 0.04$	1.284
500	$14.48 \pm 0.06$ (68%)	0.99	$1.81 \pm 0.09$ (32%)	$0.51 \pm 0.01$	1.212
550	$13.57 \pm 0.11$ (57%)	$0.96 \pm 0.01$	$0.52 \pm 0.08$ (43%)	$0.45 \pm 0.03$	1.041
600	$11.85 \pm 0.25$ (50%)	0.90	$0.47 \pm 0.13$ (50%)	$0.55 \pm 0.10$	0.929

<sup>a</sup>Fractional amplitude with PL lifetime.

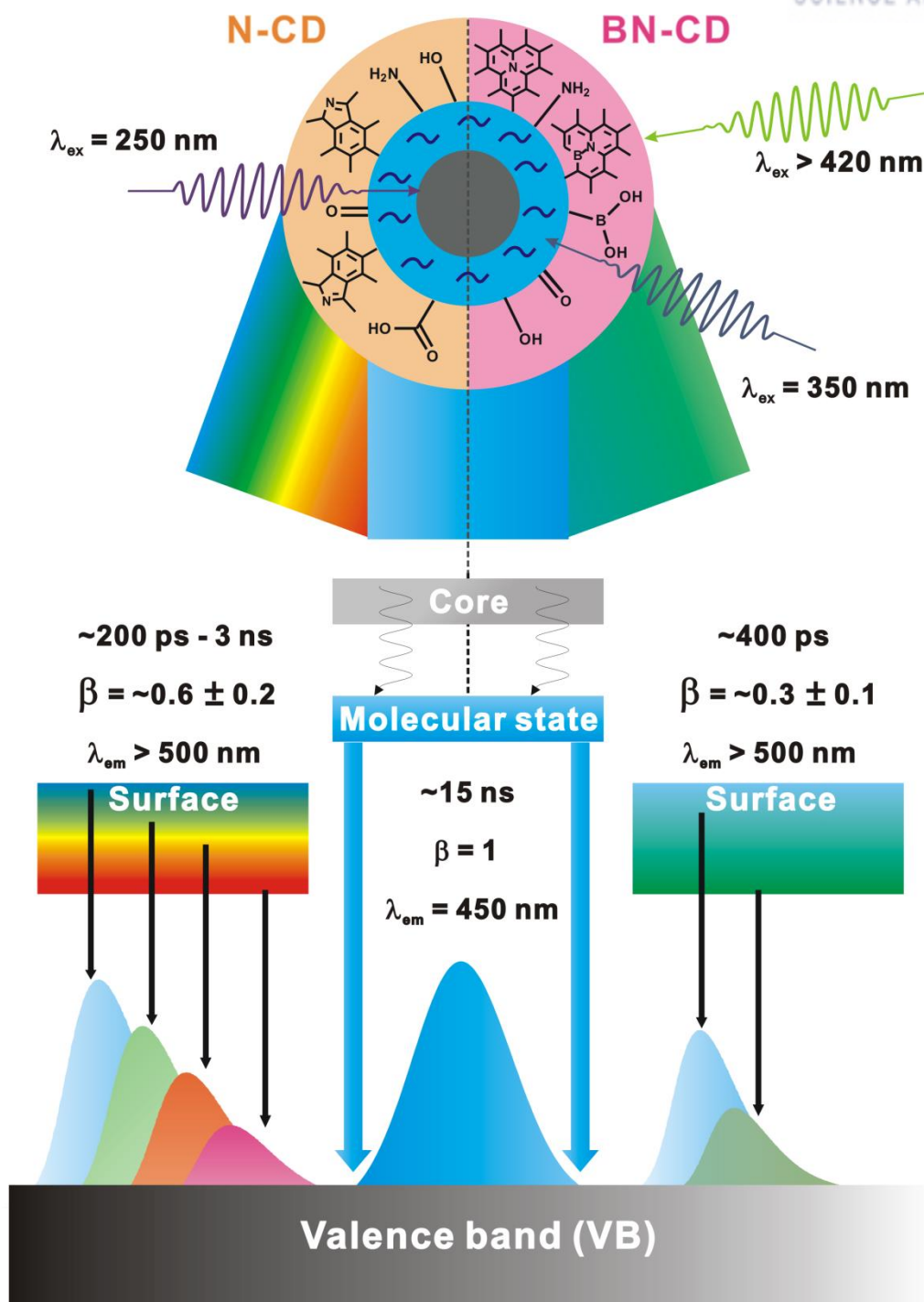
<sup>b</sup>Distribution parameter according to stretched exponential function.

**Table 2.** Fitting parameters of PL decay of BN-CD with excitation at 375 nm.

BN-CD					
$\lambda_{\text{em}}$ (nm)	$\tau_1$ (ns)	$\beta_1$	$\tau_2$ (ns)	$\beta_2$	$\chi^2$
450	$14.90 \pm 0.05$ (93%) <sup>a</sup>	$1.00 \pm 0.01^b$	$2.14 \pm 0.13$ (7%)	$0.35 \pm 0.01$	1.289
500	$15.17 \pm 0.06$ (83%)	$1.00 \pm 0.01$	$0.42 \pm 0.04$ (17%)	$0.31 \pm 0.01$	1.071
550	$15.27 \pm 0.13$ (73%)	$1.00 \pm 0.01$	$0.28 \pm 0.10$ (27%)	$0.36 \pm 0.03$	1.000
600	$14.99 \pm 0.43$ (62%)	$1.00 \pm 0.03$	$0.38 \pm 0.13$ (38%)	$0.31 \pm 0.02$	1.033

<sup>a</sup>Fractional amplitude with PL lifetime.

<sup>b</sup>Distribution parameter according to stretched exponential function.



**Scheme 1.** Proposed PL mechanism of both CDs.

## References

1. Jeong, J.; Cho, M.; Lim, Y. T.; Song, N. W.; Chung, B. H., Synthesis and characterization of a photoluminescent nanoparticle based on fullerene-silica hybridization. *Angew Chem Int Ed Engl* **2009**, *48* (29), 5296-9.
2. Welsher, K.; Liu, Z.; Sherlock, S. P.; Robinson, J. T.; Chen, Z.; Daranciang, D.; Dai, H., A route to brightly fluorescent carbon nanotubes for near-infrared imaging in mice. *Nat Nanotechnol* **2009**, *4* (11), 773-80.
3. Geim, A. K.; Novoselov, K. S., The rise of graphene. *Nat Mater* **2007**, *6* (3), 183-91.
4. Baker, S. N.; Baker, G. A., Luminescent carbon nanodots: emergent nanolights. *Angew Chem Int Ed Engl* **2010**, *49* (38), 6726-44.
5. Derfus, A. M.; Chan, W. C. W.; Bhatia, S. N., Probing the Cytotoxicity of Semiconductor Quantum Dots. *Nano Letters* **2004**, *4* (1), 11-18.
6. Heinlaan, M.; Ivask, A.; Blinova, I.; Dubourguier, H. C.; Kahru, A., Toxicity of nanosized and bulk ZnO, CuO and TiO<sub>2</sub> to bacteria *Vibrio fischeri* and crustaceans *Daphnia magna* and *Thamnocephalus platyurus*. *Chemosphere* **2008**, *71* (7), 1308-16.
7. Li, X.; Rui, M.; Song, J.; Shen, Z.; Zeng, H., Carbon and Graphene Quantum Dots for Optoelectronic and Energy Devices: A Review. *Advanced Functional Materials* **2015**, *25* (31), 4929-4947.
8. Li, Y.; Hu, Y.; Zhao, Y.; Shi, G.; Deng, L.; Hou, Y.; Qu, L., An electrochemical avenue to green-luminescent graphene quantum dots as potential electron-acceptors for photovoltaics. *Adv Mater* **2011**, *23* (6), 776-80.
9. Zhu, S.; Zhang, J.; Tang, S.; Qiao, C.; Wang, L.; Wang, H.; Liu, X.; Li, B.; Li, Y.; Yu, W.; Wang, X.; Sun, H.; Yang, B., Surface Chemistry Routes to Modulate the Photoluminescence of Graphene Quantum Dots: From Fluorescence Mechanism to Up-Conversion Bioimaging Applications. *Advanced Functional Materials* **2012**, *22* (22), 4732-4740.
10. Qian, Z.; Ma, J.; Shan, X.; Shao, L.; Zhou, J.; Chen, J.; Feng, H., Surface functionalization of graphene quantum dots with small organic molecules from photoluminescence modulation to bioimaging applications: an experimental and theoretical investigation. *RSC Advances* **2013**, *3* (34), 14571.
11. Li, H.; He, X.; Kang, Z.; Huang, H.; Liu, Y.; Liu, J.; Lian, S.; Tsang, C. H.; Yang, X.; Lee, S. T., Water-soluble fluorescent carbon quantum dots and photocatalyst design. *Angew Chem Int Ed Engl* **2010**, *49* (26), 4430-4.
12. Ding, C.; Zhu, A.; Tian, Y., Functional surface engineering of C-dots for fluorescent biosensing and in vivo bioimaging. *Acc Chem Res* **2014**, *47* (1), 20-30.
13. Wang, Q.; Huang, X.; Long, Y.; Wang, X.; Zhang, H.; Zhu, R.; Liang, L.; Teng, P.; Zheng, H.,

Hollow luminescent carbon dots for drug delivery. *Carbon* **2013**, 59, 192-199.

14. Wang, C.; Wu, X.; Li, X.; Wang, W.; Wang, L.; Gu, M.; Li, Q., Upconversion fluorescent carbon nanodots enriched with nitrogen for light harvesting. *Journal of Materials Chemistry* **2012**, 22 (31), 15522.
15. Choi, Y.; Kang, B.; Lee, J.; Kim, S.; Kim, G. T.; Kang, H.; Lee, B. R.; Kim, H.; Shim, S.-H.; Lee, G.; Kwon, O.-H.; Kim, B.-S., Integrative Approach toward Uncovering the Origin of Photoluminescence in Dual Heteroatom-Doped Carbon Nanodots. *Chemistry of Materials* **2016**, 28 (19), 6840-6847.
16. Qu, D.; Zheng, M.; Zhang, L.; Zhao, H.; Xie, Z.; Jing, X.; Haddad, R. E.; Fan, H.; Sun, Z., Formation mechanism and optimization of highly luminescent N-doped graphene quantum dots. *Sci Rep* **2014**, 4, 5294.
17. Li, X.; Zhang, S.; Kulinich, S. A.; Liu, Y.; Zeng, H., Engineering surface states of carbon dots to achieve controllable luminescence for solid-luminescent composites and sensitive Be<sup>2+</sup> detection. *Scientific Reports* **2014**, 4.
18. Zhang, Y.-Q.; Ma, D.-K.; Zhuang, Y.; Zhang, X.; Chen, W.; Hong, L.-L.; Yan, Q.-X.; Yu, K.; Huang, S.-M., One-pot synthesis of N-doped carbon dots with tunable luminescence properties. *Journal of Materials Chemistry* **2012**, 22 (33), 16714.
19. Dong, Y.; Pang, H.; Yang, H. B.; Guo, C.; Shao, J.; Chi, Y.; Li, C. M.; Yu, T., Carbon-based dots co-doped with nitrogen and sulfur for high quantum yield and excitation-independent emission. *Angew Chem Int Ed Engl* **2013**, 52 (30), 7800-4.
20. Liu, Y.; Liu, C.-y.; Zhang, Z.-y., Graphitized carbon dots emitting strong green photoluminescence. *Journal of Materials Chemistry C* **2013**, 1 (32), 4902.
21. Feng, Y.; Zhao, J.; Yan, X.; Tang, F.; Xue, Q., Enhancement in the fluorescence of graphene quantum dots by hydrazine hydrate reduction. *Carbon* **2014**, 66, 334-339.
22. Barman, M. K.; Jana, B.; Bhattacharyya, S.; Patra, A., Photophysical Properties of Doped Carbon Dots (N, P, and B) and Their Influence on Electron/Hole Transfer in Carbon Dots–Nickel (II) Phthalocyanine Conjugates. *The Journal of Physical Chemistry C* **2014**, 118 (34), 20034-20041.
23. Zhao, Q. L.; Zhang, Z. L.; Huang, B. H.; Peng, J.; Zhang, M.; Pang, D. W., Facile preparation of low cytotoxicity fluorescent carbon nanocrystals by electrooxidation of graphite. *Chem Commun (Camb)* **2008**, (41), 5116-8.
24. Zheng, L.; Chi, Y.; Dong, Y.; Lin, J.; Wang, B., Electrochemiluminescence of Water-Soluble Carbon Nanocrystals Released Electrochemically from Graphite. *J. am. chem. soc* **2009**, 131, 4564-4565.
25. Zhou, J.; Booker, C.; Li, R.; Zhou, X.; Sham, T. K.; Sun, X.; Ding, Z., An electrochemical avenue to blue luminescent nanocrystals from multiwalled carbon nanotubes (MWCNTs). *J Am Chem Soc* **2007**, 129 (4), 744-5.

26. Cao, L.; Wang, X.; Meziani, M. J.; Lu, F.; Wang, H.; Luo, P. G.; Lin, Y.; Harruff, B. A.; Veca, L. M.; Murray, D.; Xie, S. Y.; Sun, Y. P., Carbon dots for multiphoton bioimaging. *J Am Chem Soc* **2007**, *129* (37), 11318-9.
27. Hu, S.-L.; Niu, K.-Y.; Sun, J.; Yang, J.; Zhao, N.-Q.; Du, X.-W., One-step synthesis of fluorescent carbon nanoparticles by laser irradiation. *J. Mater. Chem.* **2009**, *19* (4), 484-488.
28. Sun, Y. P.; Wang, X.; Lu, F.; Cao, L.; Meziani, M. J.; Luo, P. G.; Gu, L.; Veca, L. M., Doped Carbon Nanoparticles as a New Platform for Highly Photoluminescent Dots. *J Phys Chem C Nanomater Interfaces* **2008**, *112* (47), 18295-18298.
29. Sun, Y. P.; Zhou, B.; Lin, Y.; Wang, W.; Fernando, K. A.; Pathak, P.; Meziani, M. J.; Harruff, B. A.; Wang, X.; Wang, H.; Luo, P. G.; Yang, H.; Kose, M. E.; Chen, B.; Veca, L. M.; Xie, S. Y., Quantum-sized carbon dots for bright and colorful photoluminescence. *J Am Chem Soc* **2006**, *128* (24), 7756-7.
30. Wang, X.; Cao, L.; Lu, F.; Meziani, M. J.; Li, H.; Qi, G.; Zhou, B.; Harruff, B. A.; Kermarrec, F.; Sun, Y. P., Photoinduced electron transfers with carbon dots. *Chem Commun (Camb)* **2009**, (25), 3774-6.
31. Yang, S. T.; Wang, X.; Wang, H.; Lu, F.; Luo, P. G.; Cao, L.; Meziani, M. J.; Liu, J. H.; Liu, Y.; Chen, M.; Huang, Y.; Sun, Y. P., Carbon Dots as Nontoxic and High-Performance Fluorescence Imaging Agents. *J Phys Chem C Nanomater Interfaces* **2009**, *113* (42), 18110-18114.
32. Xu, X.; Ray, R.; Gu, Y.; Ploehn, H. J.; Gearheart, L.; Raker, K.; Scrivens, W. A., Electrophoretic analysis and purification of fluorescent single-walled carbon nanotube fragments. *J Am Chem Soc* **2004**, *126* (40), 12736-7.
33. Yang, Z. C.; Wang, M.; Yong, A. M.; Wong, S. Y.; Zhang, X. H.; Tan, H.; Chang, A. Y.; Li, X.; Wang, J., Intrinsically fluorescent carbon dots with tunable emission derived from hydrothermal treatment of glucose in the presence of monopotassium phosphate. *Chem Commun (Camb)* **2011**, 47 (42), 11615-7.
34. Sahu, S.; Behera, B.; Maiti, T. K.; Mohapatra, S., Simple one-step synthesis of highly luminescent carbon dots from orange juice: application as excellent bio-imaging agents. *Chem Commun (Camb)* **2012**, 48 (70), 8835-7.
35. Zhu, H.; Wang, X.; Li, Y.; Wang, Z.; Yang, F.; Yang, X., Microwave synthesis of fluorescent carbon nanoparticles with electrochemiluminescence properties. *Chem Commun (Camb)* **2009**, (34), 5118-20.
36. Wang, X.; Qu, K.; Xu, B.; Ren, J.; Qu, X., Microwave assisted one-step green synthesis of cell-permeable multicolor photoluminescent carbon dots without surface passivation reagents. *Journal of Materials Chemistry* **2011**, *21* (8), 2445.
37. Dhenadhayalan, N.; Lin, K.-C.; Suresh, R.; Ramamurthy, P., Unravelling the Multiple Emissive States in Citric-Acid-Derived Carbon Dots. *The Journal of Physical Chemistry C* **2016**, *120*



(2), 1252-1261.

38. Gan, Z.; Xiong, S.; Wu, X.; Xu, T.; Zhu, X.; Gan, X.; Guo, J.; Shen, J.; Sun, L.; Chu, P. K., Mechanism of Photoluminescence from Chemically Derived Graphene Oxide: Role of Chemical Reduction. *Advanced Optical Materials* **2013**, *1* (12), 926-932.
39. Wang, L.; Zhu, S. J.; Wang, H. Y.; Qu, S. N.; Zhang, Y. L.; Zhang, J. H.; Chen, Q. D.; Xu, H. L.; Han, W.; Yang, B.; Sun, H. B., Common origin of green luminescence in carbon nanodots and graphene quantum dots. *ACS Nano* **2014**, *8* (3), 2541-7.
40. Liu, F.; Jang, M. H.; Ha, H. D.; Kim, J. H.; Cho, Y. H.; Seo, T. S., Facile synthetic method for pristine graphene quantum dots and graphene oxide quantum dots: origin of blue and green luminescence. *Adv Mater* **2013**, *25* (27), 3657-62.
41. Bao, L.; Zhang, Z. L.; Tian, Z. Q.; Zhang, L.; Liu, C.; Lin, Y.; Qi, B.; Pang, D. W., Electrochemical tuning of luminescent carbon nanodots: from preparation to luminescence mechanism. *Adv Mater* **2011**, *23* (48), 5801-6.
42. Krysmann, M. J.; Kellarakis, A.; Dallas, P.; Giannelis, E. P., Formation mechanism of carbogenic nanoparticles with dual photoluminescence emission. *J Am Chem Soc* **2012**, *134* (2), 747-50.
43. Zhang, X. F.; Shao, X.; Liu, S., Dual fluorescence of graphene oxide: a time-resolved study. *J Phys Chem A* **2012**, *116* (27), 7308-13.
44. Hao, Y.; Gan, Z.; Zhu, X.; Li, T.; Wu, X.; Chu, P. K., Emission from Trions in Carbon Quantum Dots. *The Journal of Physical Chemistry C* **2015**, *119* (6), 2956-2962.
45. Pan, D.; Zhang, J.; Li, Z.; Wu, C.; Yan, X.; Wu, M., Observation of pH-, solvent-, spin-, and excitation-dependent blue photoluminescence from carbon nanoparticles. *Chem Commun (Camb)* **2010**, *46* (21), 3681-3.
46. Zhang, W.; Liu, Y.; Meng, X.; Ding, T.; Xu, Y.; Xu, H.; Ren, Y.; Liu, B.; Huang, J.; Yang, J.; Fang, X., Graphenol defects induced blue emission enhancement in chemically reduced graphene quantum dots. *Phys Chem Chem Phys* **2015**, *17* (34), 22361-6.
47. Chien, C. T.; Li, S. S.; Lai, W. J.; Yeh, Y. C.; Chen, H. A.; Chen, I. S.; Chen, L. C.; Chen, K. H.; Nemoto, T.; Isoda, S.; Chen, M.; Fujita, T.; Eda, G.; Yamaguchi, H.; Chhowalla, M.; Chen, C. W., Tunable photoluminescence from graphene oxide. *Angew Chem Int Ed Engl* **2012**, *51* (27), 6662-6.
48. Zheng, C.; An, X.; Gong, J., Novel pH sensitive N-doped carbon dots with both long fluorescence lifetime and high quantum yield. *RSC Adv.* **2015**, *5* (41), 32319-32322.
49. Nie, H.; Li, M.; Li, Q.; Liang, S.; Tan, Y.; Sheng, L.; Shi, W.; Zhang, S. X.-A., Carbon Dots with Continuously Tunable Full-Color Emission and Their Application in Ratiometric pH Sensing. *Chemistry of Materials* **2014**, *26* (10), 3104-3112.
50. Bhattacharya, A.; Chatterjee, S.; Prajapati, R.; Mukherjee, T. K., Size-dependent penetration of carbon dots inside the ferritin nanocages: evidence for the quantum confinement effect in carbon



dots. *Phys Chem Chem Phys* **2015**, *17* (19), 12833-40.

51. Hao, Y.; Gan, Z.; Xu, J.; Wu, X.; Chu, P. K., Poly(ethylene glycol)/carbon quantum dot composite solid films exhibiting intense and tunable blue–red emission. *Applied Surface Science* **2014**, *311*, 490-497.
52. Shang, J.; Ma, L.; Li, J.; Ai, W.; Yu, T.; Gurzadyan, G. G., The origin of fluorescence from graphene oxide. *Sci Rep* **2012**, *2*, 792.
53. Zhu, S.; Meng, Q.; Wang, L.; Zhang, J.; Song, Y.; Jin, H.; Zhang, K.; Sun, H.; Wang, H.; Yang, B., Highly photoluminescent carbon dots for multicolor patterning, sensors, and bioimaging. *Angew Chem Int Ed Engl* **2013**, *52* (14), 3953-7.
54. Song, Y.; Zhu, S.; Zhang, S.; Fu, Y.; Wang, L.; Zhao, X.; Yang, B., Investigation from chemical structure to photoluminescent mechanism: a type of carbon dots from the pyrolysis of citric acid and an amine. *J. Mater. Chem. C* **2015**, *3* (23), 5976-5984.
55. Wang, Y.; Kalytchuk, S.; Zhang, Y.; Shi, H.; Kershaw, S. V.; Rogach, A. L., Thickness-Dependent Full-Color Emission Tunability in a Flexible Carbon Dot Ionogel. *J Phys Chem Lett* **2014**, *5* (8), 1412-20.
56. Reckmeier, C. J.; Wang, Y.; Zboril, R.; Rogach, A. L., Influence of Doping and Temperature on Solvatochromic Shifts in Optical Spectra of Carbon Dots. *The Journal of Physical Chemistry C* **2016**, *120* (19), 10591-10604.
57. Wang, H.; Sun, P.; Cong, S.; Wu, J.; Gao, L.; Wang, Y.; Dai, X.; Yi, Q.; Zou, G., Nitrogen-Doped Carbon Dots for "green" Quantum Dot Solar Cells. *Nanoscale Res Lett* **2016**, *11* (1), 27.
58. Röding, M.; Bradley, S. J.; Nydén, M.; Nann, T., Fluorescence Lifetime Analysis of Graphene Quantum Dots. *The Journal of Physical Chemistry C* **2014**, *118* (51), 30282-30290.

## Acknowledgements

I thank Dr. Yuri Choi at UNIST for providing the samples and their element chemical analysis. I also appreciate my advisor, Prof. Oh-Hoon Kwon, for giving me a great opportunity to complete my thesis. Without his encouragement and support in the research, I could not complete my research. This work supported by the NRF Korea funded by the Ministry of Science, ICT and Future Planning (MSIP) (2014R1A1A1008289). I also appreciate all of group members in our lab for continuous encouragement for my research.